

AD-A014365

AFFDL-TR-75-24

## TRANSIENT CALORIMETER CALIBRATION SYSTEM

TAMARACK SCIENTIFIC COMPANY  
ORANGE, CALIFORNIA

TECHNICAL REPORT AFFDL-TR-75-24

MARCH 1975

FINAL REPORT FOR PERIOD MARCH 1973 - FEBRUARY 1974

Approved for public release; distribution unlimited.

AIR FORCE FLIGHT DYNAMICS LABORATORY  
AIR FORCE SYSTEMS COMMAND  
WRIGHT-PATTERSON AIR FORCE BASE, OHIO 45433

20070917055

## NOTICE

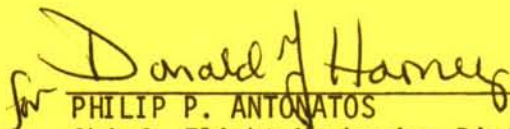
When Government drawings, specifications, or other data are used for any purpose other than in connection with a definitely related Government procurement operation, the United States Government thereby incurs no responsibility nor any obligation whatsoever; and the fact that the government may have formulated, furnished, or in any way supplied the said drawings, specifications, or other data, is not to be regarded by implication or otherwise as in any manner licensing the holder or any other person or corporation, or conveying any rights or permission to manufacture, use, or sell any patented invention that may in any way be related thereto.

This technical report has been reviewed and is approved for publication.



WILLIAM E. ALEXANDER  
Research and Development Group  
Experimental Engineering Branch

FOR THE COMMANDER:



PHILIP P. ANTONATOS  
Chief, Flight Mechanics Division  
Air Force Flight Dynamics Laboratory

Copies of this report should not be returned unless return is required by security considerations, contractual obligations, or notice on a specific document.

UNCLASSIFIED

SECURITY CLASSIFICATION OF THIS PAGE (When Data Entered)

REPORT DOCUMENTATION PAGE		READ INSTRUCTIONS BEFORE COMPLETING FORM
1. REPORT NUMBER  AFFDI-TR-75-24	2. GOVT ACCESSION NO.	3. RECIPIENT'S CATALOG NUMBER
4. TITLE (and Subtitle)  TRANSIENT CALORIMETER CALIBRATION SYSTEM		5. TYPE OF REPORT & PERIOD COVERED FINAL 1 Mar 73 to 1 Feb 74
		6. PERFORMING ORG. REPORT NUMBER
7. AUTHOR(s) R.E. Sheets R.L. Pierce		8. CONTRACT OR GRANT NUMBER(s)  F33615-73-C-3045
9. PERFORMING ORGANIZATION NAME AND ADDRESS Tamarack Scientific Company Incorporated 231 Emerson Avenue Orange, California 92667		10. PROGRAM ELEMENT, PROJECT, TASK AREA & WORK UNIT NUMBERS 62201F 14260124
11. CONTROLLING OFFICE NAME AND ADDRESS Flight Mechanics Division Air Force Flight Dynamics Laboratory Wright-Patterson AFB, Ohio 45433		12. REPORT DATE March 1975
14. MONITORING AGENCY NAME & ADDRESS (if different from Controlling Office)		13. NUMBER OF PAGES 55
		15. SECURITY CLASS. (of this report)  UNCLASSIFIED
		15a. DECLASSIFICATION/DOWNGRADING SCHEDULE
16. DISTRIBUTION STATEMENT (of this Report)  Approved for public release; distribution unlimited.		
17. DISTRIBUTION STATEMENT (of the abstract entered in Block 20, if different from Report)		
18. SUPPLEMENTARY NOTES		
19. KEY WORDS (Continue on reverse side if necessary and identify by block number) calibration facilities; calorimeters; radiometer; electric arcs; images; absorption coefficients; xenon lamps; heat flux measurement; atmosphere entry test facility		
20. ABSTRACT (Continue on reverse side if necessary and identify by block number) Null point calorimeters are used to measure heat flux levels in excess of 15.0 kW/cm <sup>2</sup> in arc heated re-entry wind tunnels. To augment these measurements at the Air Force Flight Dynamics Laboratory a calibration system and a transfer standard was developed. The system generates heat flux densities up to 10 kW/cm <sup>2</sup> within a 0.25 in square target zone using a xenon arc radiation source. The absorptivity of calorimeter surfaces to this radiant source is measured with an accessory apparatus to yield a calibration accuracy of 5%.		

UNCLASSIFIED

SECURITY CLASSIFICATION OF THIS PAGE (When Data Entered)



## FOREWORD

This report was prepared by Tamarack Scientific Company of Orange, California, and summarizes their work under Contract F33615-73-C-3045. The developments reported were carried out under Project 1426, "Experimental Simulation of Flight Mechanics," Task 142601, "Diagnostic, Instrumentation and Similitude Technology," and work unit 14260124, "Development of a Calibrator for 15,000 Btu/sq ft-s Heat Flux Gages used during ground tests of AF Re-entry vehicles Models." Mr. William E. Alexander of the Air Force Flight Dynamics Laboratory (AFFDL/FXN) was the contract monitor.

This development effort was initiated in March, 1973, and was completed in February, 1974.

The technical report was released by the authors in March, 1974, for publication.

## TABLE OF CONTENTS

<u>Section</u>		
I	INTRODUCTION	1
	1. Objective	1
	2. Approach	2
	3. General Program Description	3
II	GENERAL DESCRIPTION OF RADIANT SOURCE AND DEVELOPMENT TECHNOLOGY	5
III	LAMP MODULE	8
IV	COLLECTOR DESIGN	9
V	OPTICAL INTEGRATOR	12
VI	HIGH INTENSITY APERTURES	20
VII	HIGH SPEED SHUTTER	22
VIII	TRANSFER STANDARD	24
	1. General Description and Theory of Operation	24
	2. Design Calculations	25
	3. Radiometer Test	30
	4. Error Analysis of the Cavity Radiometer	31
IX	ABSORPTIVITY DEVICE	33
	1. Description and Design	33
	2. Error Analysis of the Absorptivity Device	36
X	COPPER MELT TEST DATA	39
XI	SAMPLE MOUNT AND TEST PROVISIONS	43
XII	OVERALL SYSTEM PERFORMANCE	46

## LIST OF ILLUSTRATIONS

<u>Figure</u>		<u>Page</u>
1	Optical Layout. . . . .	6
2	Rotated Ellipse Collector Contour . . . . .	10
3	Optical Integrator. . . . .	13
4	Optical System. . . . .	14
5	Optical Integrator. . . . .	15
6	Integrator Uniformity . . . . .	18
7	Area of Uniform Intensity from Optical Integrator . . . .	19
8	High Intensity Aperture . . . . .	21
9	High Speed Shutter. . . . .	23
10	Transfer Standard Cavity Radiometer . . . . .	26
11	Cavity Radiometer Modes of Operation. . . . .	27
12	Radiometer Aperture . . . . .	29
13	Absorptivity Layout . . . . .	34
14	Mounting Configuration, Copper Rod Melt Test. . . . .	40
15	Null Point Calorimeter Mount. . . . .	44
16	Table Assembly. . . . .	45
17	Uniform Heat Flux . . . . .	47
18	Maximum System Heat Flux. . . . .	48
19	System Components . . . . .	50

## SECTION I

### INTRODUCTION

#### 1. OBJECTIVE

The objective of the program was to develop a calibration system to calibrate transient (null point) calorimeters. Transient null point calorimeters are most commonly being used to measure heat transfer rates to a solid body immersed in a high pressure, high enthalpy, flowing gas stream. These gas streams produced by re-entry arc heated wind tunnels, produce stagnation heat flux levels in excess of  $15 \text{ kW/cm}^2$ . Currently null point calorimeter heat flux measurements are based on mathematical analysis since conventional calibration facilities produce an intensity of only  $0.5 \text{ kW/cm}^2$ , which is far too low for accurate data extrapolation.

Calibration of null point calorimeters requires a system which can produce more than an order of magnitude increase over conventional calibration facilities. This system must also have the following:

- a. A source of uniform heat flux to excite the null point calorimeter during calibration.
- b. A method to provide for nearly instantaneous exposure at the start of a test and to control the duration of heat flux applied to prevent damage (melting) of the calorimeter.

c. A transfer standard to accurately measure the incident heat flux used to excite the null point calorimeter with traceability to secondary standards.

## 2. APPROACH

These requirements were met by utilizing a radiant beam to provide the heat flux. Radiant energy provides true surface heating without damage. The four listed characteristics were met as follows:

a. Heat flux for null point calorimeter excitation is provided by a high pressure xenon plasma arc lamp, ellipsoidal aluminum mirror and an optical integrator to provide a uniform beam of radiant energy.

b. Duration of the beam energy applied to the calorimeter is controlled by a high speed shutter located upstream of the optical integrator.

c. A cavity radiometer transfer standard is used to measure the beam incident heat flux. This radiometer consists of a small (0.125 in diameter) water cooled aperture through which radiation enters. Radiation is absorbed on the blackened cavity walls, heating the cavity. Heat transfer by conduction from the cavity to a water cooled heat sink is measured by a differential thermopile. Calibration is provided by heating the cavity wall with an electrical coil, the input to which can be accurately measured.

d. The percentage of beam radiant energy absorbed by the null point surface is obtained in a separate test by an absorptivity measuring apparatus.



### 3. GENERAL PROGRAM DESCRIPTION

Prior to 1973, Tamarack Scientific Company, Incorporated, had developed a High Intensity Thermal Radiant Heating and Calibrating facility. This facility had been used to perform quality control tests on null point calorimeters, nuclear blast thermal radiation simulation, and rocket engine heat transfer tests. The system consisted of a high pressure xenon plasma arc lamp, ellipsoidal collector, high speed shutter and cavity radiometer. With regard to null point calibration, this system could provide an incident heat flux in excess of  $8 \text{ kW/cm}^2$ ; however, it did not have an optical integrator in the system to insure uniformity of beam profile. During the quality control test on a number of null point calorimeters over a year's time, a great deal of experience was accumulated which was useful in directing the development of the calibration system.

Based on this work, research and development was continued in the following areas to improve the system performance for null point calorimeter calibration and to provide a transfer standard:

- a. An increase in beam energy flux
- b. The development of an optical integrator to provide four percent uniformity over a  $0.25 \text{ in} \times 0.25 \text{ in}$  target area.
- c. The design of a cavity radiometer aperture which can withstand the high heat flux levels encountered during calibration.

d. The verification of absorptivity of a colloidal graphite coating used on calibrator components.

e. The performance of a copper melt test to verify and correlate system performance.

f. The performance of error analysis on the entire calibration process.

## SECTION II

### GENERAL DESCRIPTION OF RADIANT SOURCE AND DEVELOPMENT TECHNOLOGY

The radiant heat flux system consists of a xenon plasma arc lamp as the power source and an ellipsoidal collector to focus the energy past a high speed shutter onto an optical integrator consisting of precision chamfered segments which form a square tube with reflecting internal surfaces. The focused beam passes by multiple reflection through the integrator, producing a beam of uniform cross section at the exit aperture. A simplified optical layout is shown in Figure 1.

The transfer standard is an electrically calibrated cavity radiometer, used to measure the flux density, as described briefly in Section I.

The absorptivity measuring device is somewhat similar in operation to the cavity radiometer in that it utilizes a differential thermocouple to monitor heat flow. The unit is mounted on the side of the xenon lamphouse and utilizes a small fraction of the lamp power for measurement of null point calorimeter surface absorptivity.

Basically, the development work performed covers the following summarized areas:

- a. The optimization of a high efficiency collector to maximize beam intensity.
- b. The development of an optical integrator capable of providing good uniformity and withstanding high heat flux levels.

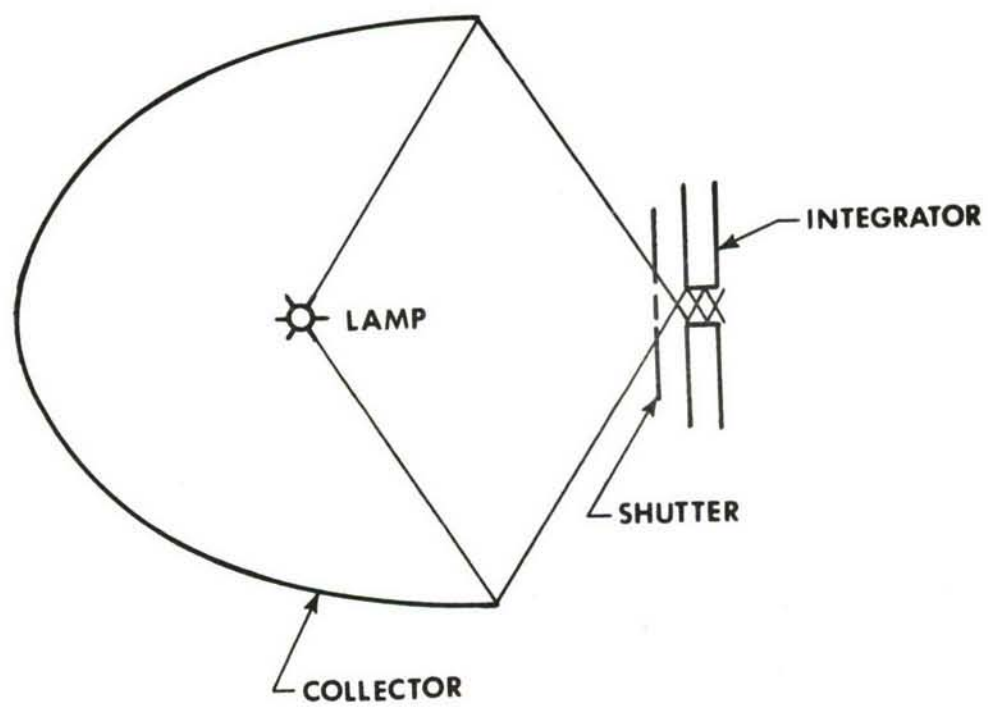


Figure 1 Optical Layout



c. The upgrading of the cavity radiometer aperture to withstand extremely high power levels.

d. The development of an absorptivity device to provide measurement data of calorimeter surface absorptivity.

The following sections of this report cover the development, performance, and error analysis of the above mentioned items, as well as the significant state-of-the-art problem areas encountered in the design and assembly work. This report concludes with a summary of the system performance and a brief description of the improved calibration system.

## SECTION III

### LAMP MODULE

The power source of the calibration system is a Tamarack Scientific Company, Incorporated, Model JP-50 jet-pinched xenon plasma arc lamp. Its characteristics are covered briefly here because of its intimate relation to the design of the collector.

In the jet pinched arc source the xenon is circulated through the lamp and is utilized to form a high velocity axial flow around the arc discharge from cathode to anode. The controlled jet flow has a number of effects on the arc discharge. It positively positions the arc on the axis of the lamp, constricts the discharge in the region of the cathode to increase radiancy, increases operating voltage to provide higher power, and stabilizes the arc anode foot in a concave cup to increase footing area which decreases the heat loading on the anode.

The arc is trumpet shaped with the highest radiance in the region of the cathode where its size is small. Further from the cathode the radiance becomes lower and the arc diameter is larger. When the product of the average magnification of the collector and the arc length is larger than the target size (the integrator entrance aperture) the target will be overfilled. The collector design must be optimized to project the maximum amount of energy onto the target focal plane.

## SECTION IV

### COLLECTOR DESIGN

The collector is designed to concentrate the highest radiance portion of the arc on the focal plane. To accomplish this, the collector contour is generated by revolving an ellipse, which has been rotated about one focus, about the major axis of its original position. This revolution occurs, then, about the optical axis of the collector. The tip of the cathode and the periphery of the focal plane become the major axis focal points. The cathode tip produces a circular ring at the periphery of the focal plane, the highest radiance portion of the arc is concentrated and averaged over the focal plane, and the anode is allowed to spill over in a larger concentric ring. This is illustrated in Figure 2.

Optimization of the collector contour was determined by a parametric study of the intensity as a function of the major axis and focal lengths and the cone angle while holding a fixed diameter value of 22 inches. The results of the study yielded a cone angle of  $110^\circ$  for maximum efficiency.

The collector was machined from a forged billet of aluminum material to a template generated by a computer program and a tape controlled milling machine to produce the required contour. After machining, the collector was nickel plated, ground, polished, aluminized, and overcoated with  $\text{MgF}_2$ .  $\text{MgF}_2$  is used to prevent oxidation and provides

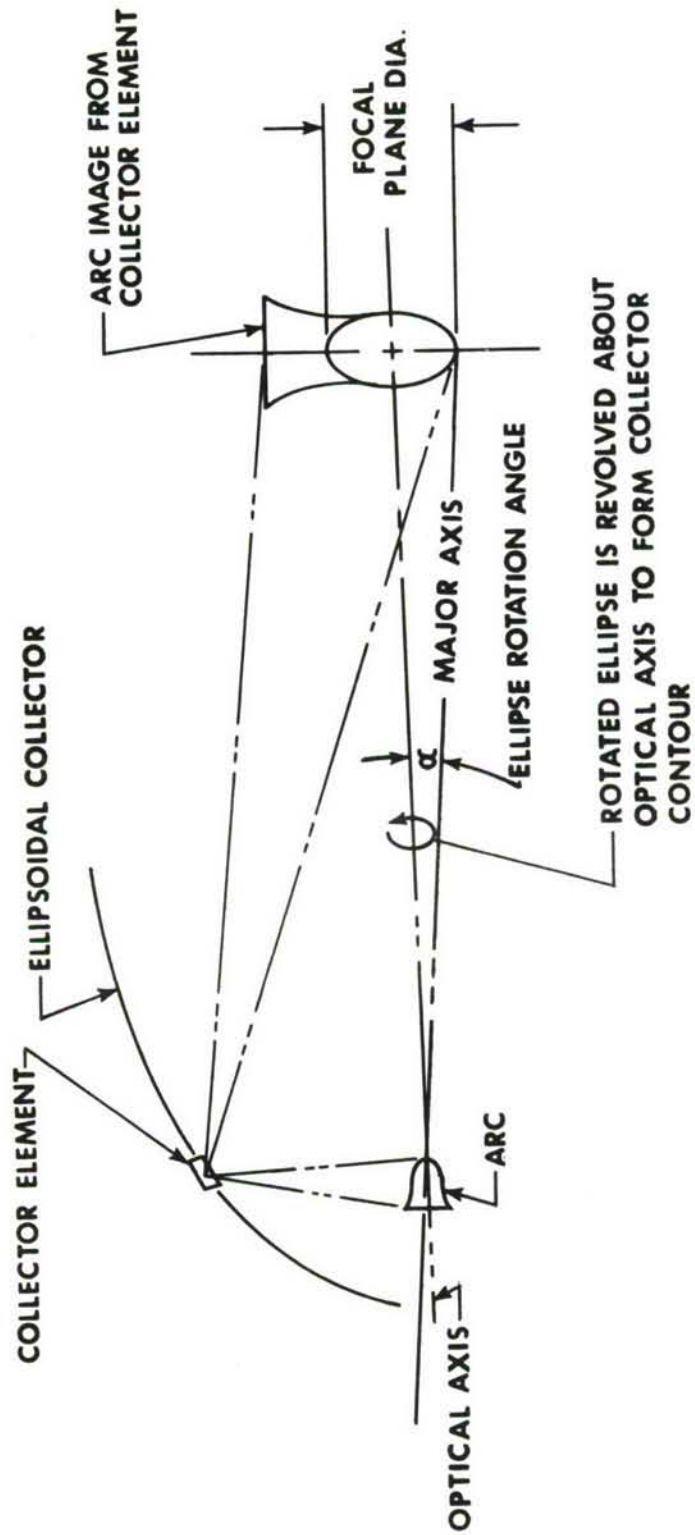


Figure 2 Rotated Ellipse Collector Contour



a rugged surface which can be cleaned. Copper cooling coils were then applied to the external surface of the collector and bonded with thermally conductive aluminum-filled Devcon epoxy.

## SECTION V

### OPTICAL INTEGRATOR

The purpose of the optical integrator is to accept the high intensity radiation of the focal plane and provide a highly uniform intensity pattern at the exit aperture. Uniformity of beam intensity is accomplished as a result of the radiation undergoing multiple reflections within the device.

The integrator consists of four precision chamfered segments that are joined together to form a square channel as shown in Figure 3. The reflective surfaces of the copper segments are nickel plated, ground, polished, aluminumized and magnesium fluoride overcoated, the entire device is water cooled.

The integrator is positioned with the entrance aperture at the focal plane of the arc image as shown in Figure 4. If the integrator were not present, the energy would diverge and illuminate an area of radius "R" (See Figure 5). The effect of the integrator is to subdivide this area into square segments of area equal to that of the integrator and superimpose these segments at the exit aperture. The degree of uniformity is limited only by the length of the integrator and the resulting number of reflections undergone within the device. In a system where the output heat flux must be high, the integrator should be no longer than necessary to provide the desired uniformity so that energy losses due to reflections can be minimized. The number

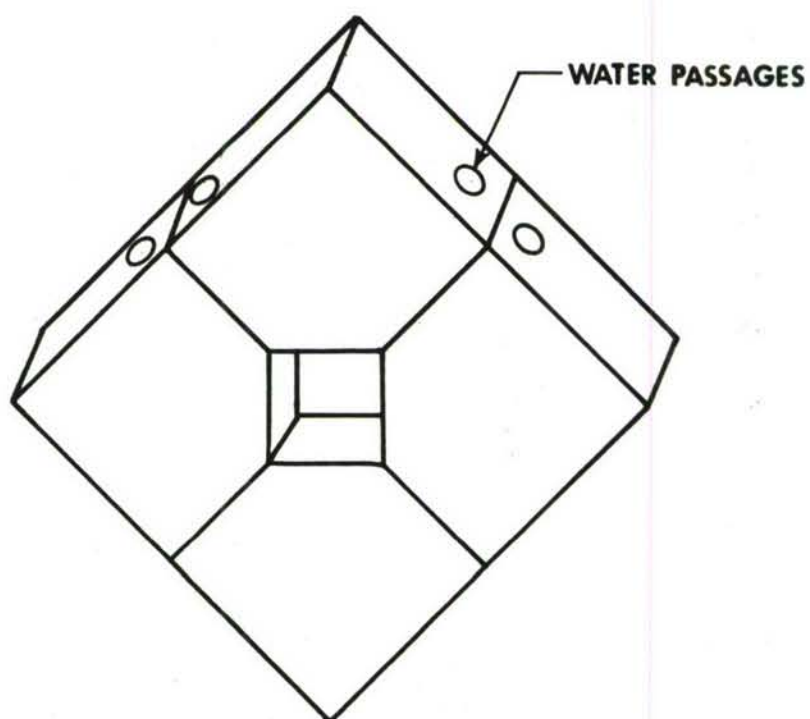


Figure 3 Optical Integrator

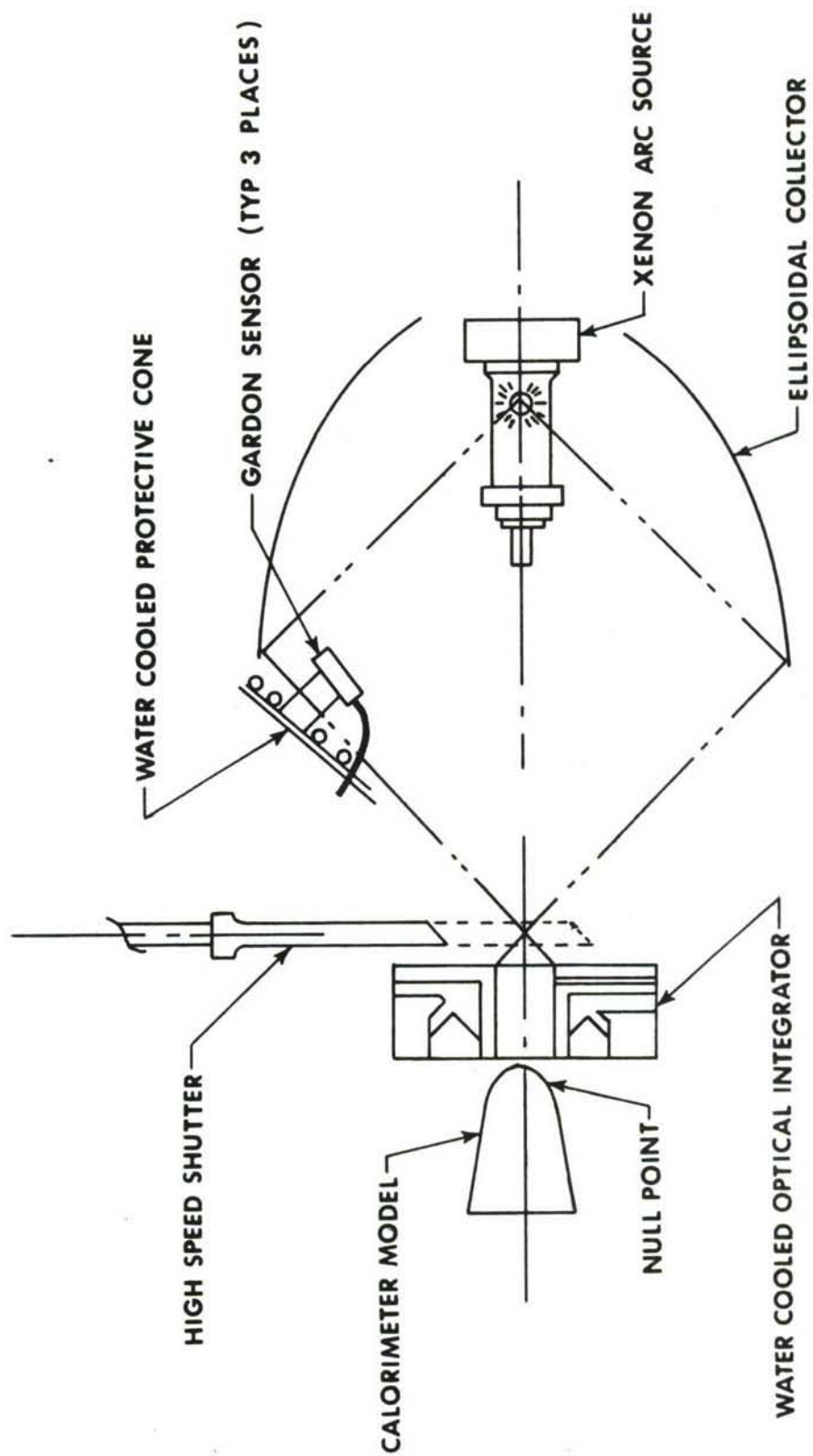


Figure 4 Optical System



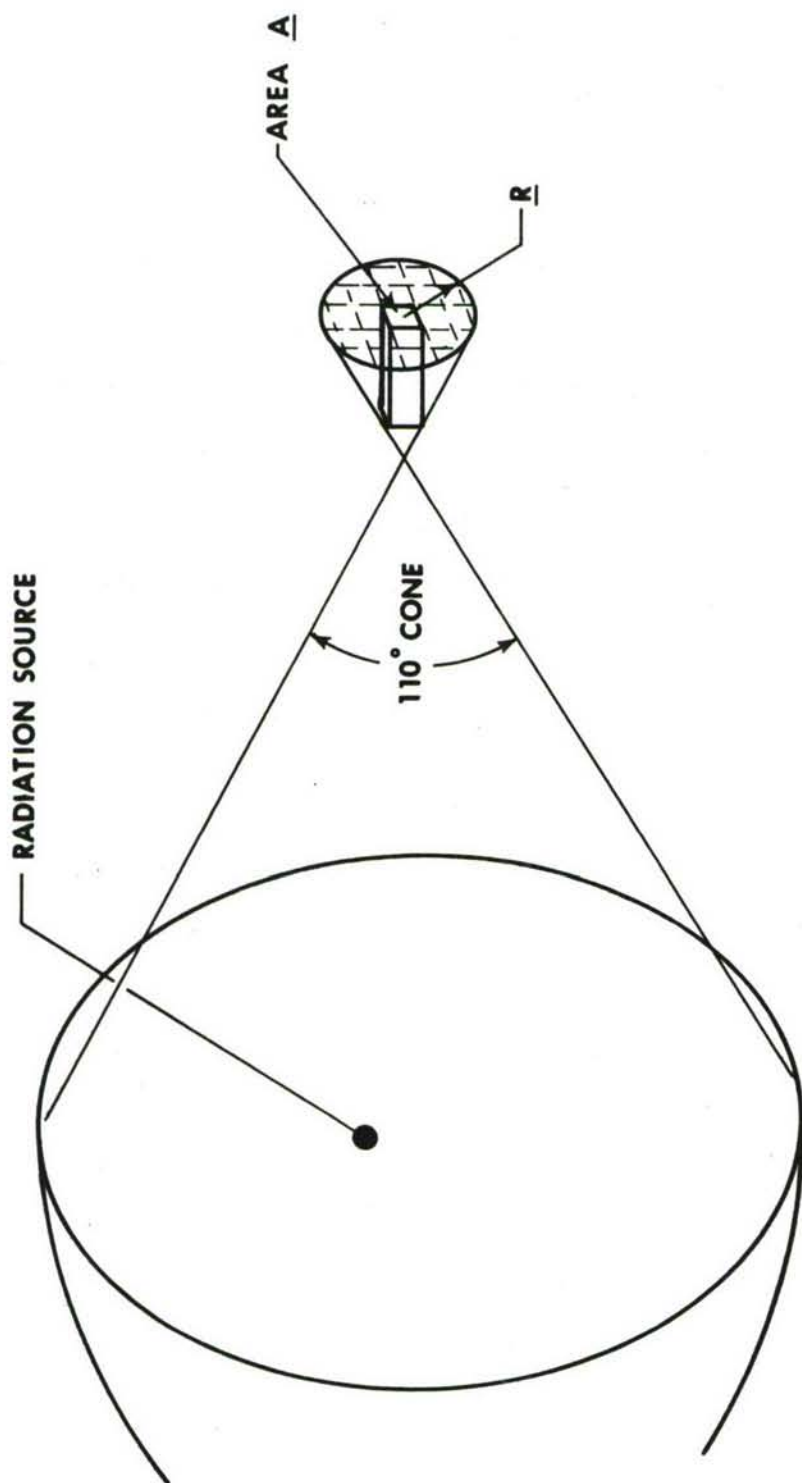


Figure 5 Optical Integrator

of squares produced in the subdividing process is related to the number of internal reflections by the relation  $N = (2F + 1)^2$ , where  $F$  is the number of reflections. Three reflections produces 49 superimposed areas.

Several sizes and lengths were built to provide various target plane areas and evaluate intensity and uniformity characteristics. They ranged from 0.25 in X 0.25 in to 0.50 in X 0.50 in and up to 0.70 in long, providing up to three internal reflections. An important feature of this integrator design is that the exit area is accurately defined and the total radiant energy passing through the exit can be measured in a cavity receiver. This provides an additional check on the incident heat flux generated by the system.

It was found that the combination of uniformity and intensity of the output beam is a strong function of lamp focusing. An increase in uniformity may be obtained at the expense of maximum intensity by slight axial defocusing. A uniformity scan is, in fact, a good method of verifying proper lamp focus. For optimum results, the detector should be significantly smaller than the integrator exit aperture.

As this type detector is not readily available for continuous high intensities, the system radiometer was used to perform a uniformity scan on a 0.25 in X 0.25 in square integrator. Since the radiometer aperture was .125 in diameter, a certain amount of averaging was inherent in the readings, and the edge reading on each side required a 2.5% compensation due to the occlusion of the radiometer

aperture by the edge of integrator. A plot of the data (both actual and compensated) is shown in Figure 6. The uniformity across the integrator aperture is about 4%.

The degree of nonuniformity in the compensated data is due to the limitation of the area of uniform distribution by virtue of the cone angle. Figure 7 illustrates the situation. The beam spread at the exit aperture is equal to the total cone angle at the entrance aperture. The area of uniform radiation is the triangle in front of the integrator exit as defined by the cone angle. The null point calorimeter must be placed within this area to insure uniform radiation exposure on the detector.

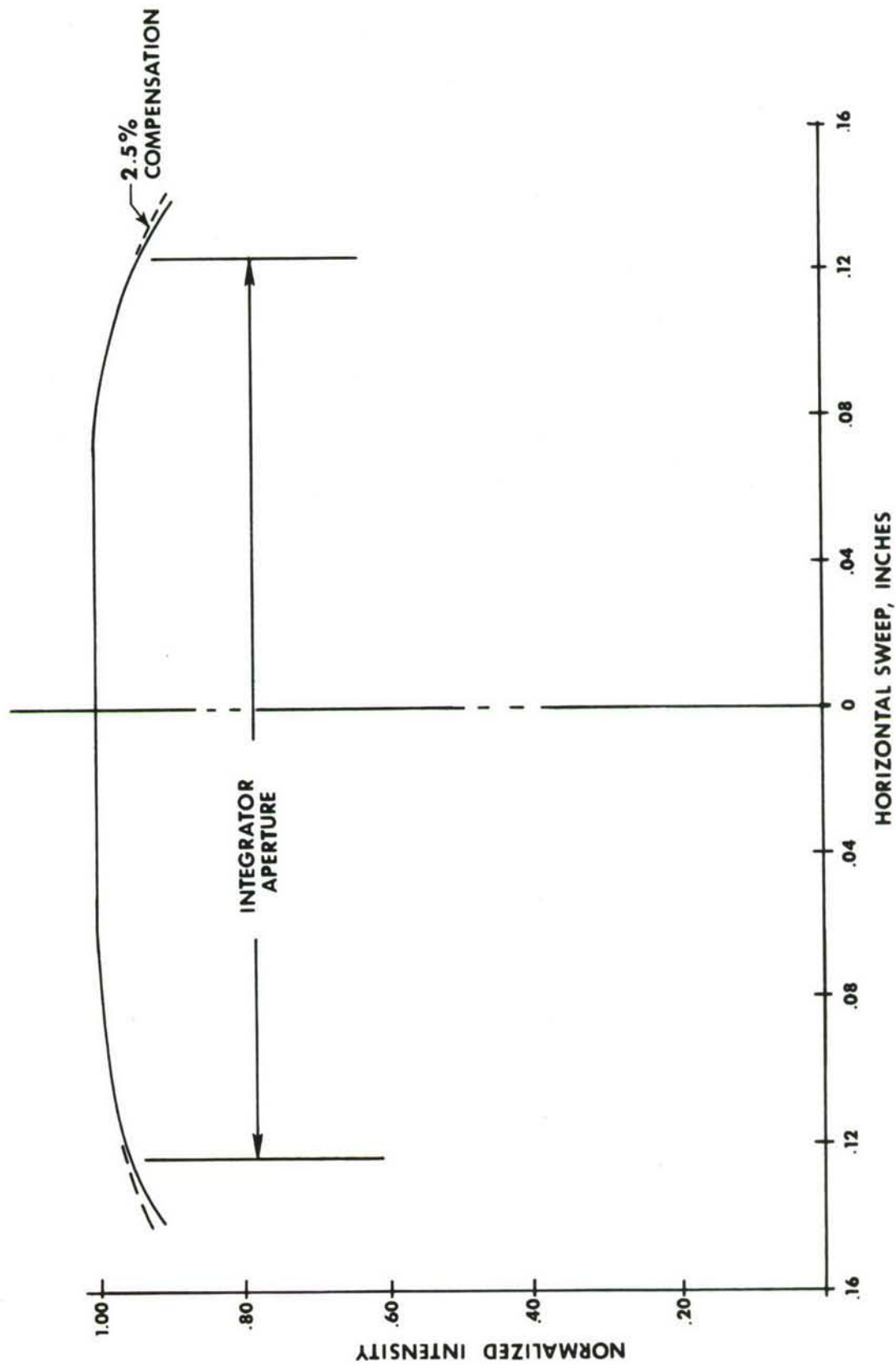


Figure 6 Integrator Uniformity

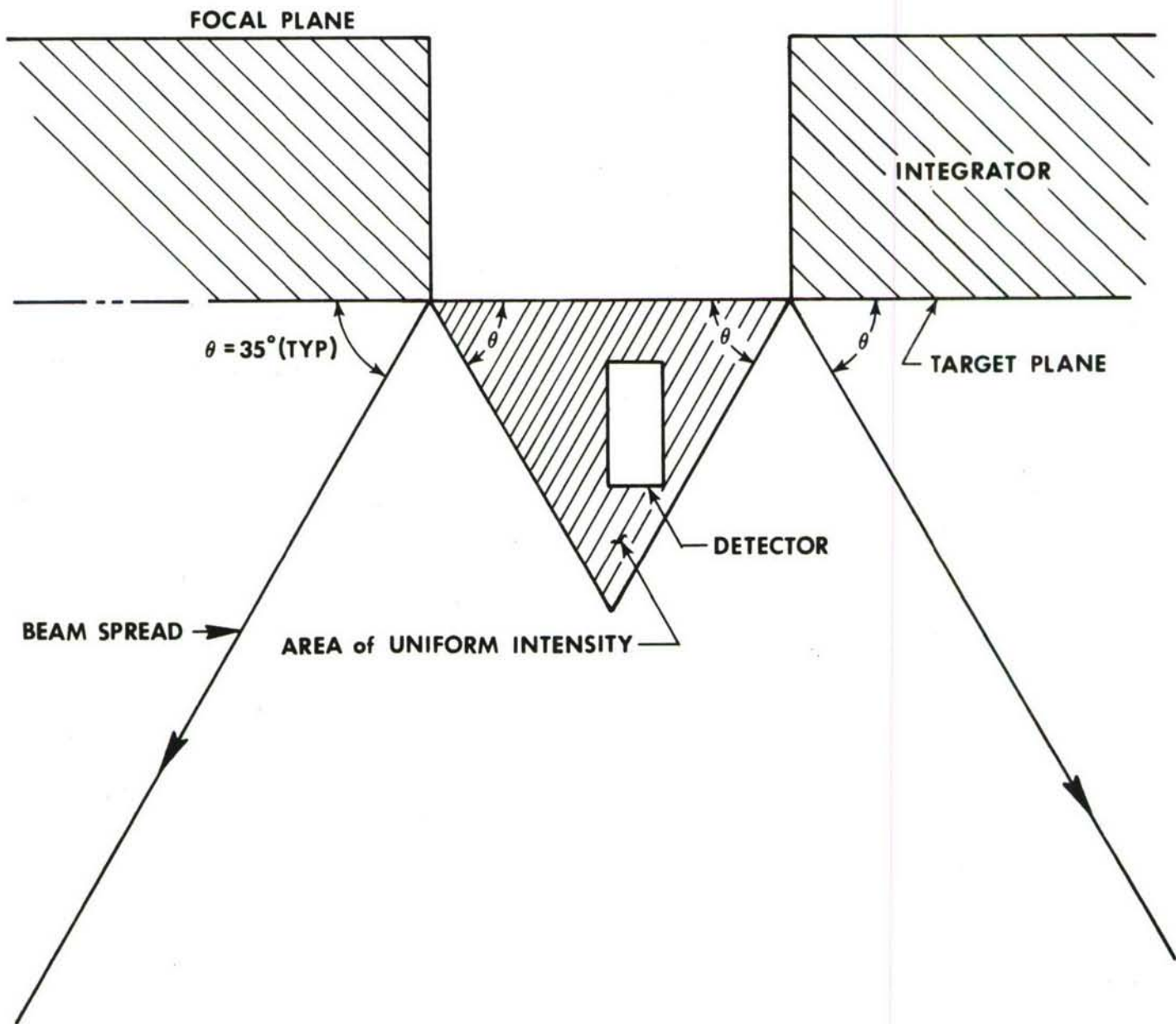


Figure 7 Area of Uniform Intensity  
from Optical Integrator



## SECTION VI

### HIGH INTENSITY APERTURES

In addition to the optical integrators used for high uniformity, several sets of interchangeable apertures were built to obtain peak radiation intensity levels. The aperture cross-section is shown in Figure 8.

The peak intensity at the center of the 0.25 in aperture was  $11,000 \text{ W/cm}^2$  at 35 kW input and will exceed  $15,000 \text{ W/cm}^2$  at full power. The intensity at the edges of the aperture is about 50% of peak.

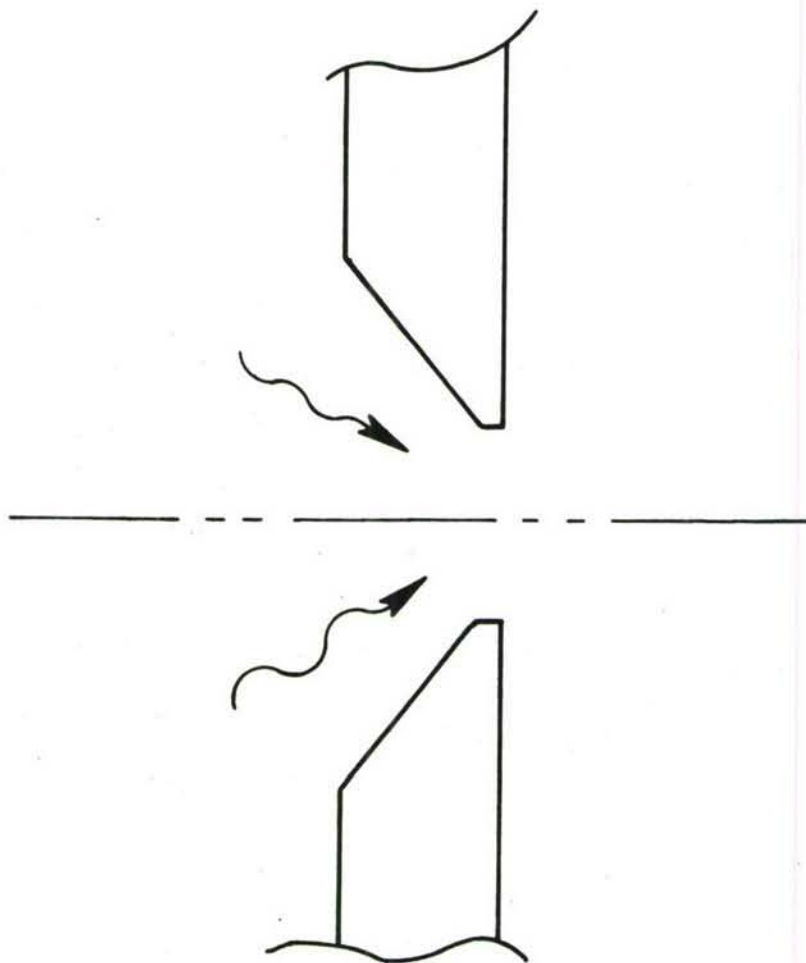


Figure 8 High Intensity Aperture

## SECTION VII

### HIGH SPEED SHUTTER

The shutter provides a means of controlling the duration of radiation exposure on the null point calorimeters. The shutter blade is located upstream of the integrator as was shown in Figure 4 and in the closed position absorbs rather than reflects the power back onto the source.

The shutter is a light weight water cooled aluminum blade driven by a pneumatically operated high pressure cylinder. The speed of the shutter is determined by the pressure of the supply, which may be 50 to 400 psig. Rise and fall times of 2 ms. have been recorded by a high speed photodiode mounted in a small pickoff port in the integrator assembly (See Figure 9).

The accumulators help enforce the driving pressure to the cylinder. Without the accumulators present, the small diameter plumbing lines would develop a significant pressure gradient and thus inhibit shutter speed.

The shutter assembly is bolted to a large energy absorption plate which is mounted on rubber shock absorbers to a steel frame.

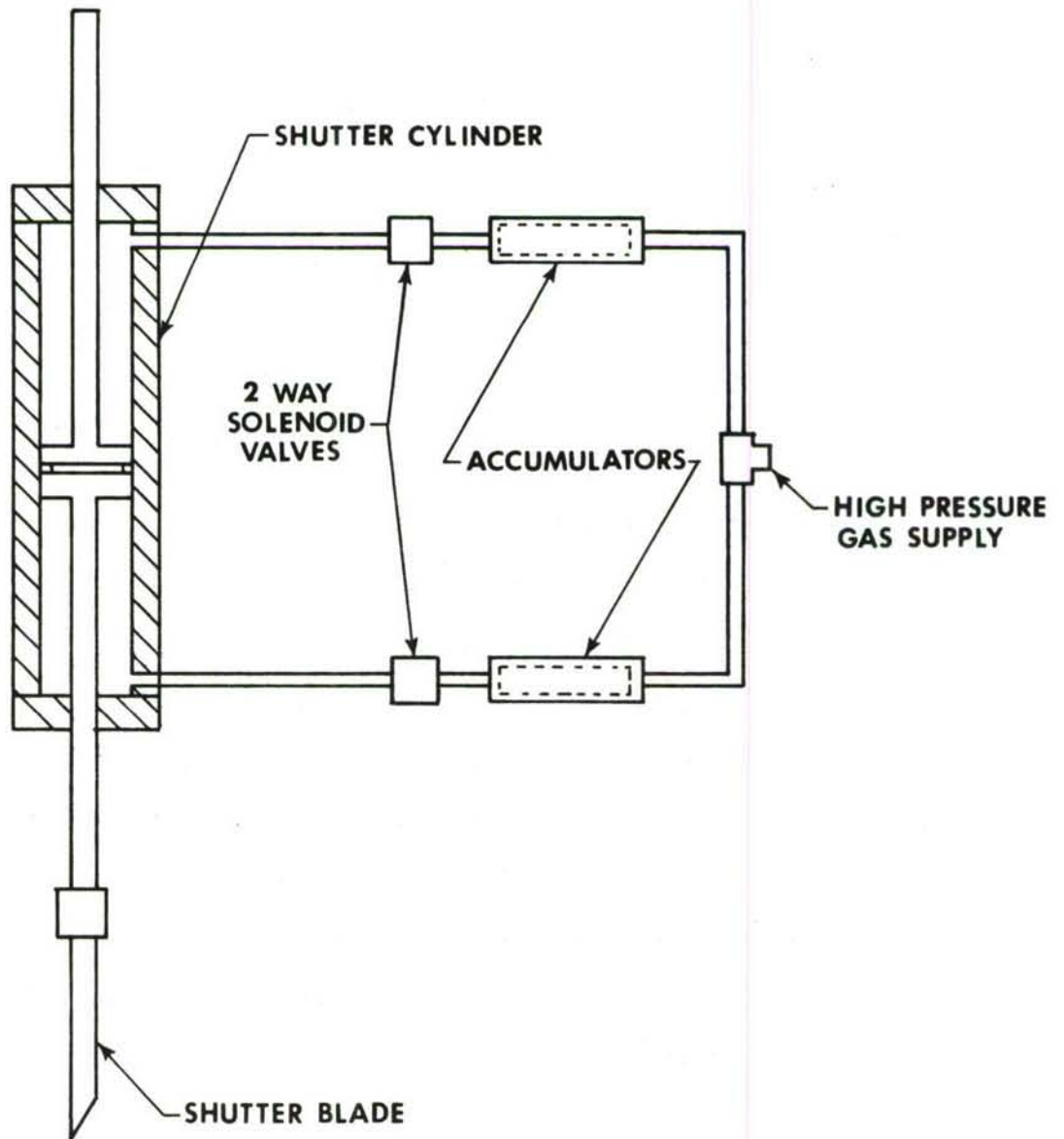


Figure 9 High Speed Shutter

## SECTION VIII

### TRANSFER STANDARD

#### 1. GENERAL DESCRIPTION AND THEORY OF OPERATION

The transfer standard is an electrically calibrated cavity radiometer which provides a convenient means of measuring incident heat flux densities. The electrical calibration feature lends to the ease with which the device may be accurately and precisely calibrated through the basic parameters of voltage and current, and length.

The radiometer is a blackbody cavity of very large internal surface area compared with the aperture area through which the power to be measured is received. The wall opposite the aperture is grooved, and all internal surfaces are blackened. Incoming radiation gives up virtually all of its energy to these walls after only two or three reflections. Energy losses through the aperture are negligible. Nearly all losses occur by conduction from the cavity walls to a heat sink. These walls are copper and are connected to the sink by more thermally resistive material. The flow of power through this resistance is measured by monitoring the difference of temperature across its length by a differential thermopile. The thermopile output is proportional to the rate of radiant power input through the aperture after steady-state heat flow to the sink is established and is independent of the coolant temperature and flow rate for the range of temperatures which occur. Using the appropriate calibration relation, the heat flux density of the incoming radiation can be calculated by dividing the rate of power loss to the heat sink by the aperture area.



Calibration of the radiometer is accomplished by applying a known voltage and current to a length of resistance wire wound around the cavity, as shown in Figure 10. The power dissipated by the wire due to Joule heating can be calculated very accurately. A ratio of input power to the product of output signal and cavity aperture area yields the desired calibration constant. Figure 11 illustrates the calibration and measurement modes of operation of the radiometer. In both cases, the heat flow path through the resistance is the same.

Extraneous radiation and heat is prevented from entering the cavity during either mode of its operation by an insulating air space between it and water cooled housing.

## 2. DESIGN CALCULATIONS

The design considerations of the radiometer involve a number of parameters:

- a. The range of flux densities to be measured,
- b. The size of aperture than can be made compatible with machining, cooling requirements, flux densities, and allowable edge thickness,
- c. The total power input, as determined by a and b above,
- d. The size of the cavity, which must be large enough to accommodate the calibration winding, significantly larger than the aperture, and small enough to retain a reasonable time constant,
- e. The allowable operating temperatures of the cavity and calibration winding, and the trade off between and time constant.

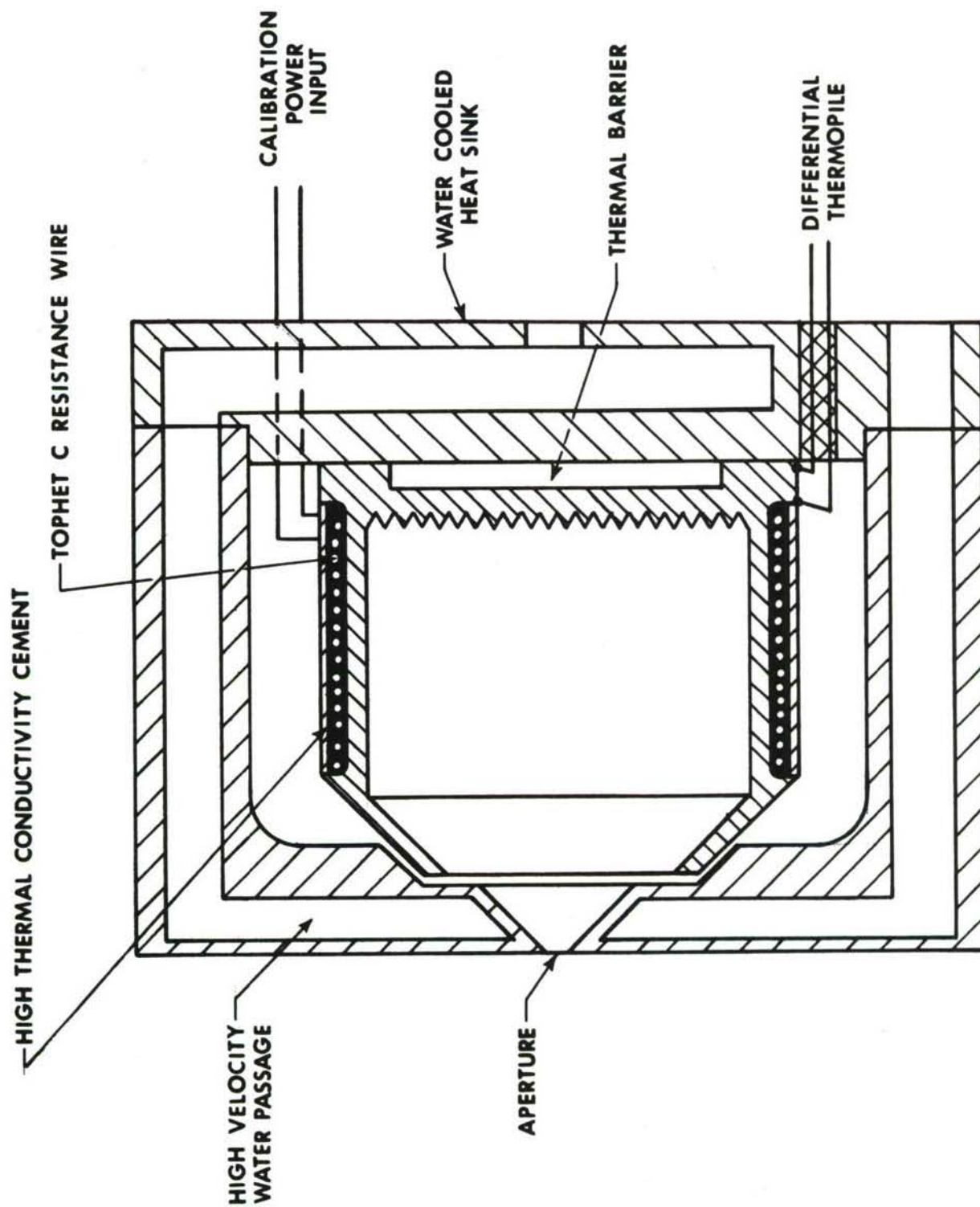


Figure 10 Transfer Standard Cavity Radiometer

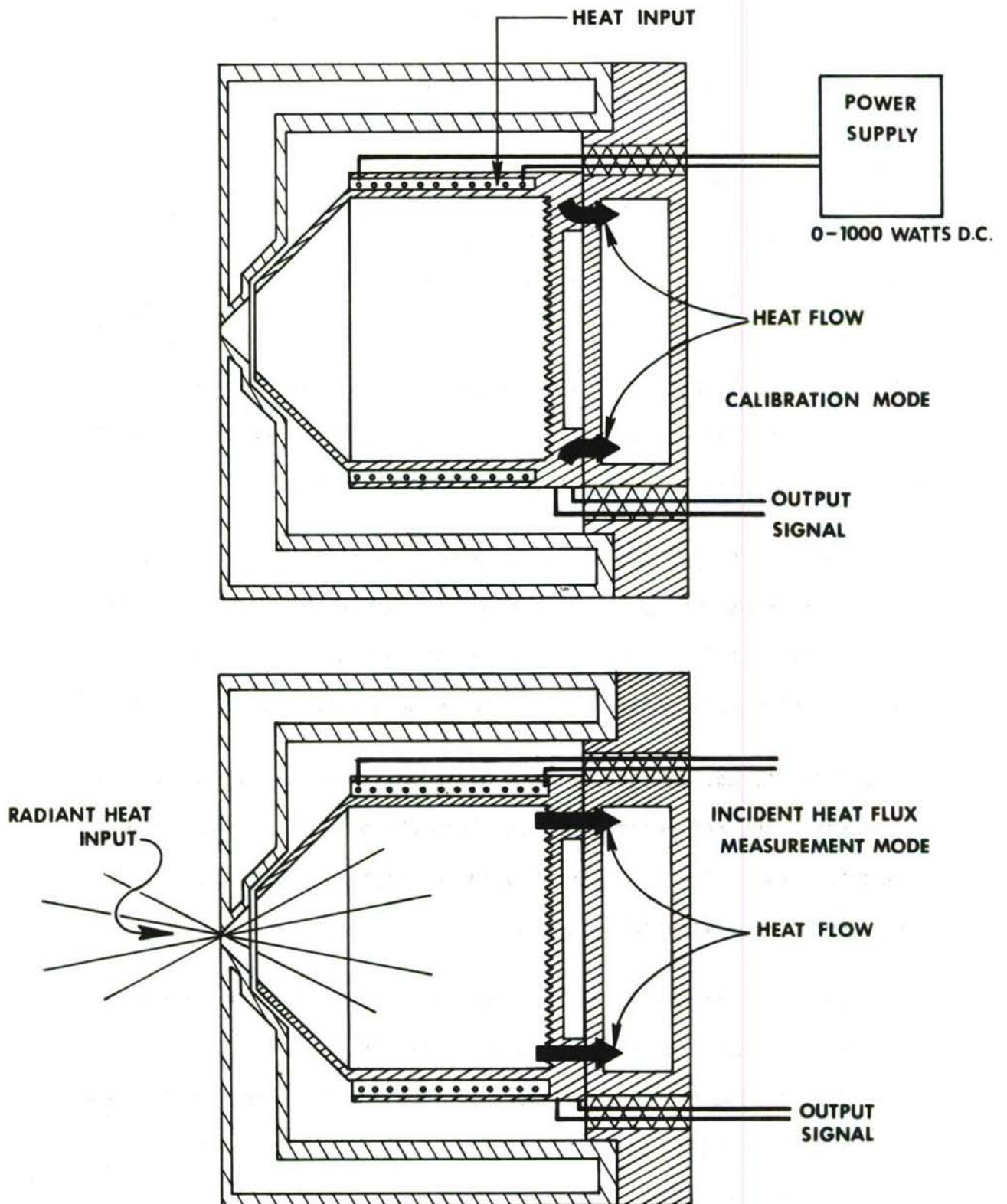


Figure 11 Cavity Radiometer Modes of Operation



The flux densities of interest range up to about  $17 \text{ kW/cm}^2$ .

In theory, the aperture should have a sharp edge with the inside walls receding at a larger angle than the incident cone angle, which in this case is  $55^\circ$ . The designed aperture has a 0.125 in diameter and a 0.015 in. thick edge (See Figure 12). Data reveals that this finite edge thickness coupled with the  $55^\circ$  cone half-angle decreases the effective size of the aperture radius about 0.006 in. The effective area is 81% of the actual area and all measured flux densities must be divided by 0.81. This value was experimentally determined and is applicable only to the particular aperture involved.

The 0.125 in aperture allows an input power of 100 W at a flux density of  $15 \text{ kW/cm}^2$ , but the possibility existed of increasing the aperture size if tests showed it could not be sufficiently cooled. The radiometer was therefore designed to be calibrated up to 2500 W.

The cavity was designed with a three in diameter serrated base to decrease the reflected intensity from the base by trapping the impinging rays. The walls are two inches high. This yielded an  $18.8 \text{ in}^2$  area for calibration winding.

A length of Tophet 'C' high temperature type resistance wire was wound over a thin coating of insulating alumina cement. Then, several thin coats of Saureisen cement were applied and thoroughly dried to prevent blistering upon application of heat. The bare wire was tightly wound on the cavity and covered with the cement and a thin copper shell. The unit was dried in a vacuum over two days.

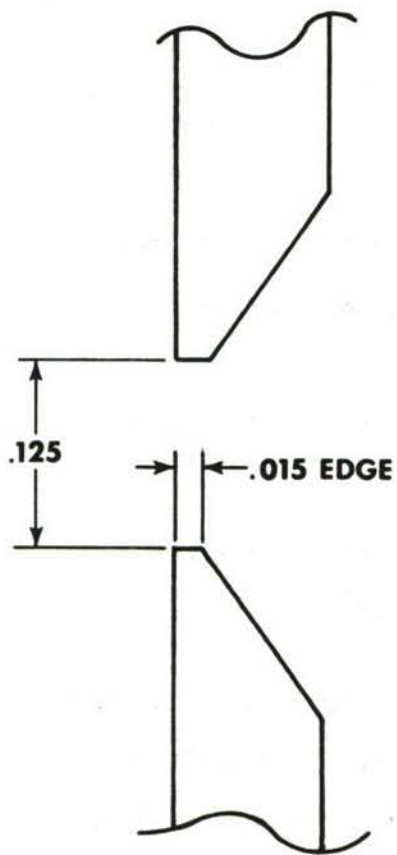


Figure 12 Radiometer Aperture



After the thermopile was installed with thermally conductive epoxy (Emerson and Cuming 2850 FT), the unit was installed in its water-cooled housing and aperture plate for tests.

### 3. RADIOMETER TEST

Calibration of the radiometer was performed up to 1000 W input and yielded a responsivity of 6.3 mv/kW and a time constant of 25 seconds. The responsivity data was quite linear, generally within  $\pm 2\%$ .

Flux density measurements were performed using the 0.25 in aperture assembly in the integrator mount. As noted in Section VI, peak flux densities of 11,000 W/cm<sup>2</sup> were recorded with the radiometer and during the copper melt test (See Section X), at an input of 35 kW. The radiometer aperture sustained some overheating during these tests but did not melt. The onset of damage threshold of the aperture appears to be about 8 kW/cm<sup>2</sup>.

Subsequent calibration tests were attempted but the pass transistors in the radiometer power control circuit were destroyed by excessive collector leakage current and the calibration winding sustained a short circuit.

A backup radiometer unit was installed in the housing and readied for test. The thermal resistance of this unit is a constantan ring which is simultaneously used as the differential thermocouple. The calibration winding is insulated with thermally conductive epoxy. Calibration could only be performed up to 340 W because of limited

capabilities of the damaged power controller. The sensitivity is 2.0 mv/kW, or 7.8 kW/cm<sup>2</sup>/mv as the compensated value for the 0.125 in diameter aperture.

#### 4. ERROR ANALYSIS OF THE CAVITY RADIOMETER

Since high heat flux standards are not available, the radiometer must be calibrated in a manner in which the active cavity is analogously excited by some source which can be or is already calibrated. The electrical calibration method employed is the most satisfactory in that the parameters are standardized.

The errors which are present include those peculiar to the voltage and current measurements, losses of energy due to unwanted conduction, radiation and convection, the nonlinearity of the thermopile, and the aperture effect. From the foregoing sections, it is intuitive that the aperture effect will contribute the largest error.

The calibration voltage and current may be measured with an accuracy of better than 0.3%. Losses due to unwanted radiation, conduction and convection can be made to cancel out by calibrating the radiometer at each input power level to be measured, because then the losses will be the same for both calibration and measurement.

The diameter of the aperture may be measured within 0.1%, but the effective aperture area has already been shown to require a correction factor of 19%.

To evaluate the aperture effect the radiometer was used first to measure the uniformity of an integrator aperture. The value, as presented earlier, was within 4%. The measured flux level was then compared to a measurement made with the radiometer without its aperture installed. Since the integrator exit aperture is well defined and the uniformity is measured, the actual value of average intensity can be calculated. The assumption made here is that the large mouth cavity actually absorbs all the energy. Since the cavity coating absorptivity is about 85%, only three reflections are required to absorb more than 99% of the total energy. The assumption is valid because the cavity base is designed to cause several reflections of a ray. Measurements were performed at several different flux levels, each one of which yielded an effective area for the radiometer aperture of 81% of the actual area. The data spread is less than 4%, and this value determines the overall accuracy of the radiometer.



## SECTION IX

### ABSORPTIVITY DEVICE

#### 1. DESCRIPTION AND DESIGN

Since the cavity radiometer measures the total incident heat flux at the target plane, it is necessary to know the fractional amount of incident heat flux which is absorbed by the null point calorimeter being calibrated. The absorptivity device performs this function.

Measurement of surface absorptivity of the calorimeter is performed at the identical spectral distribution conditions experienced during calibration when the null point calorimeter is at the primary target zone. A small pickoff port located on the cone of the lamp module samples a portion of the lamp output which is then focused by a small mirror (See Figure 13). The image is focused by a lens through the absorptivity cavity onto the surface of the detector. The cavity and its aperture are designed so that the calorimeter model being measured can be positioned in a variety of orientations to allow measurements of null point calorimeters installed at various locations on the model.

The absorptivity cavity is similar to the radiometer in that energy is monitored by means of a multiple junction thermopile arrangement, as the heat passes through four copper rods to the heat sink.

The incident energy passes through the cavity without being absorbed and strikes the null point calorimeter surface at the cavity aperture. The calorimeter is thermally isolated from the cavity so that none of the energy absorbed by it will be transmitted to the cavity. However,

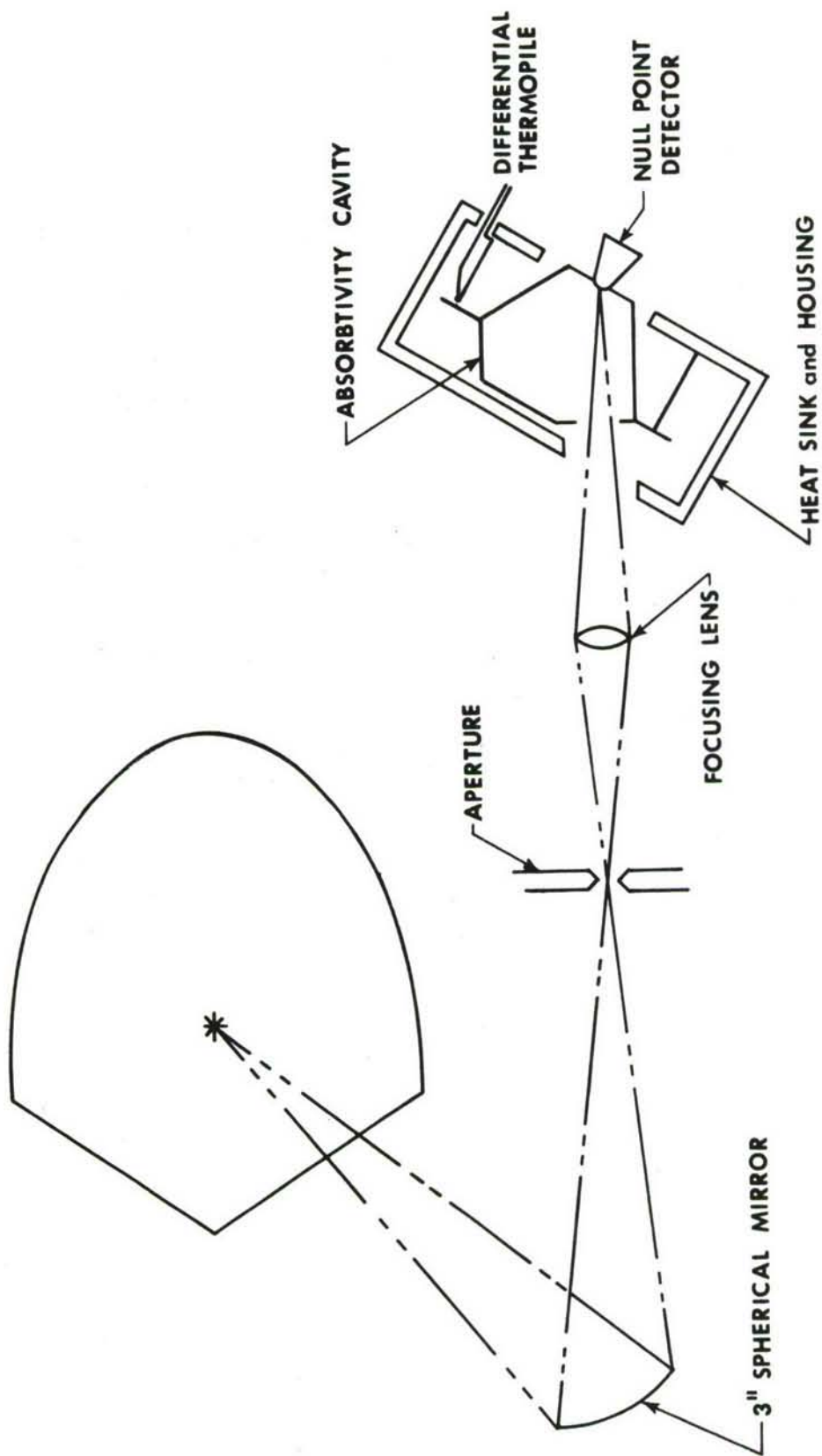


Figure 13 Absorptivity Layout



any energy that is not absorbed by the detector surface is reflected into the cavity and absorbed there. The temperature difference between the cavity and heat sink is monitored by the thermopile on a digital millivoltmeter.

In order to obtain a value for the absorptivity, the reflected energy must be compared to the total incident energy on the detector. The detector is replaced with a thermally conducting cover so that all the incident energy will be absorbed by the cover and conducted to the cavity or reflected by the cover and absorbed by the cavity. This energy is also monitored by the thermopile.

Assigning a value of  $V_1$  to the output voltage proportional to the reflected energy, and  $V_2$  to the voltage proportional to the total incident energy, the absorptivity is given as:

$$\alpha = \frac{V_2 - V_1}{V_2}$$

During calibration of the calorimeter at high flux levels, the calorimeter signal is proportional to the absorbed energy. The absorbed energy density is equal to the incident energy density, as determined by the radiometer, multiplied by the absorptivity of the detector.

Several material were evaluated for possible use on the calorimeter surface in an effort to maintain a constant value of absorptivity during high heat flux exposures. Given in Table I are absorptivity values obtained for these materials, and the results of a 0.17 second exposure at 5,800 W/cm<sup>2</sup>.

TABLE I

<u>Coating* or Material</u>	<u>Absorptivity</u>	<u>Exposure effects, 0.17 s, 5,800 W/cm<sup>2</sup></u>
1. Colloidal Graphite paint solution	.72	No visible change prior to surface melt
2. Tempil Pyromark, Type HE black paint	.84	Light grey
3. SM Nextel Black Velvet spray paint	.87	Light grey ash
4. Krylon 1602 Ultra Flat Black spray	.86	Remains black, slight grey edges
5. Rustoleum 4279 BBQ spray paint	.85	Turns grey
6. Rustoleum 412 Flat Black spray	.72	Grey-black, carbonized edges
7. Acetylene Black	.85	No visible change
8. CuO (oxidized copper)	.80	No visible change
9. 347 Stainless Steel polished	.33	No visible change
10. Polished copper	.38	No visible change

\*None of the coatings were designed to sustain the high temperatures and heat flux of these tests. No tests to evaluate the coatings for the purpose of their manufacture was made. The exposure effects can in no way be interpreted as adverse to the manufacturer's claims. The effects listed result primarily from the test method and procedures used.

The colloidal graphite remains the most promising material, closely followed by the Krylon. The black epoxy paint is believed to hold good promise but definitive tests have not been performed.

## 2. ERROR ANALYSIS OF THE ABSORPTIVITY DEVICE

Almost all the energy reflected by the calorimeter surface or reference cap is absorbed by the cavity. The energy reflected through the entrance opening is less than 2% of the total energy, while radiation and conduction of the absorbed heat from the cavity outside walls amounts to 3%. These values are proportional in the two measurements and cancel out in the final calculation of absorptivity.

The finite heat capacity of the heat sink and mount account for a 1.5% error due to the rise in temperature of the heat sink during a measurement. The nonlinearity of the thermopile contributes only 0.1%. Thus, the total error in absorptivity measurement is 1.5%.

An assumption is made that the absorptivity is independent of flux level. A change in absorptivity brought about by exposure to a high heat flux can be evaluated by measuring the absorptivity before and after exposure. Such tests performed with the colloidal graphite coating yielded no apparent change in absorptivity up through  $5 \text{ kW/cm}^2$ . In the copper melt tests, a surface prepared with colloidal graphite underwent melting with the resulting surface being oxidized. The average value of absorptivity of these two conditions yielded an incident flux density of about  $11 \text{ kW/cm}^2$ . This agreed with the radiometer measurements

within 10%. The major portion of this error being due to not knowing the exact time the surfaces melted during the 0.25 second exposure.

Taking into account the absorptivity and radiometer errors, it is reasonable to predict an overall null point calibration accuracy of 5%. Further experience, data collection, and analysis with the system should yield an even better value.



## SECTION X

### COPPER MELT TEST DATA

To help verify the available flux densities generated by the system, the method of copper melt tests was employed.

The procedure is to expose only the end face of a long thin copper rod to the high heat flux densities for just enough time to melt the surface of the face. Evaluation of the condition of the surface melt pattern is rather subjective and thus the test is somewhat lacking for objective analysis of the flux density involved. Reasonably good agreement was obtained; however, with the cavity radiometer.

A cross section of the mounting configuration of the copper rod is shown in Figure 14. The surrounding copper shield prevented radiation from striking the length of the rod.

The time required for surface melt to begin is given by the equation:

$$t_m = \frac{\pi}{4} \lambda \rho C_p \frac{(T_m - T_r)^2}{(\alpha \dot{Q})}$$

where:  $\lambda$  = the thermal conductivity, W/cm-°K

$\rho$  = the density g/cm<sup>3</sup>

$C_p$  = the specific heat, W-s/gm-°K

$T_m$  = melting temperature, °K

$T_r$  = the ambient room temperature, °K

$\dot{Q}$  = the incident flux density, W/cm<sup>2</sup>

$\alpha$  = the absorptivity



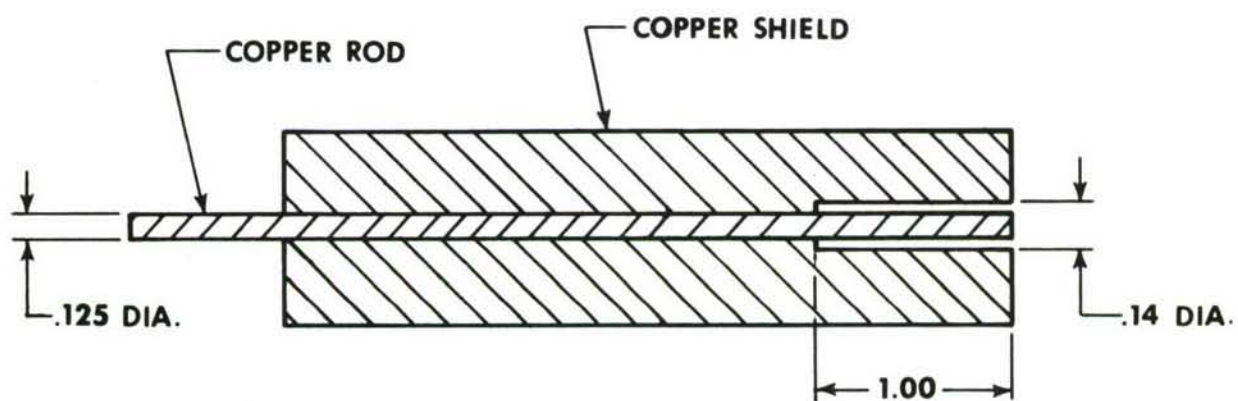


Figure 14 Mounting Configuration  
Copper Rod Melt Test

Given values  $\lambda\rho C_p = 13.81$ ,  $(T_m - T_r)^2 = 1.1266 \times 10^6$

$$t_m = \frac{1.222 \times 10^7}{(\alpha \dot{Q})}$$

It was found that the uncoated samples could be exposed more than once because the first exposure increased the absorptivity value considerably. The samples affording reliable melt patterns with a single exposure are listed below in the table of test results.

TABLE II

<u>Sample No.</u>	<u>Surface Prep.</u>	<u>Absorpt.</u>	<u>Exposure s</u>	<u>Absb. Pwr. W/cm<sup>2</sup></u>	<u>Lamp kW</u>
3B	Polished	.39	.60	4513	26
4B	Coll. Graphite	.72	.38	5671	26
5B	Polished	.39	.40	5527	33
7A	Coll. Graphite	.72	.25	6991	33
8B	Coll. Graphite	.72	.16	8739	42

The above data was obtained using the 0.25 in aperture assembly in the integrator mount.

The indicated absorbed power densities represent a minimum. Actual values will exceed those shown because the exact time that the surface melted during the exposure cannot be determined.

Calculations of the incident flux density are even more tenuous because the absorptivity values change during the exposure. This is especially true of the uncoated, polished samples.

## SECTION XI

### SAMPLE MOUNT AND TEST PROVISIONS

In order to facilitate mounting the test calorimeter model quickly and conveniently in any required orientation, a magnetic base mount was employed. The device is the type used to mount dial indicator gages on milling machine and lathe beds. The assembly is shown in Figure 15. The mount is used for both absorptivity measurements and exposure tests. The device affords easy alignment of the calorimeter model at the target plane and rigid instantaneous locking into position. The mount cannot be moved by hand when locked.

The sample table at the target plane is driven horizontally against nylon stops by a low pressure pneumatic cylinder (See Figure 16). The radiometer is mounted on the left side of the table and the test sample on the right. The mechanism allows remote control of the table to expose alternately the radiometer and test specimen to the various levels of heat flux without need for realignment.

The entire table mechanism may be retracted from the test enclosure for ease of mounting and inspecting the samples. A novel pop-up alignment device allows accurate positioning of the sample when the table is retracted. Once the sample and radiometer have been aligned with the device, the table may be inserted, driven back and forth for alternate exposures of the radiometer and test sample, and retracted for inspection without need for further realignment.

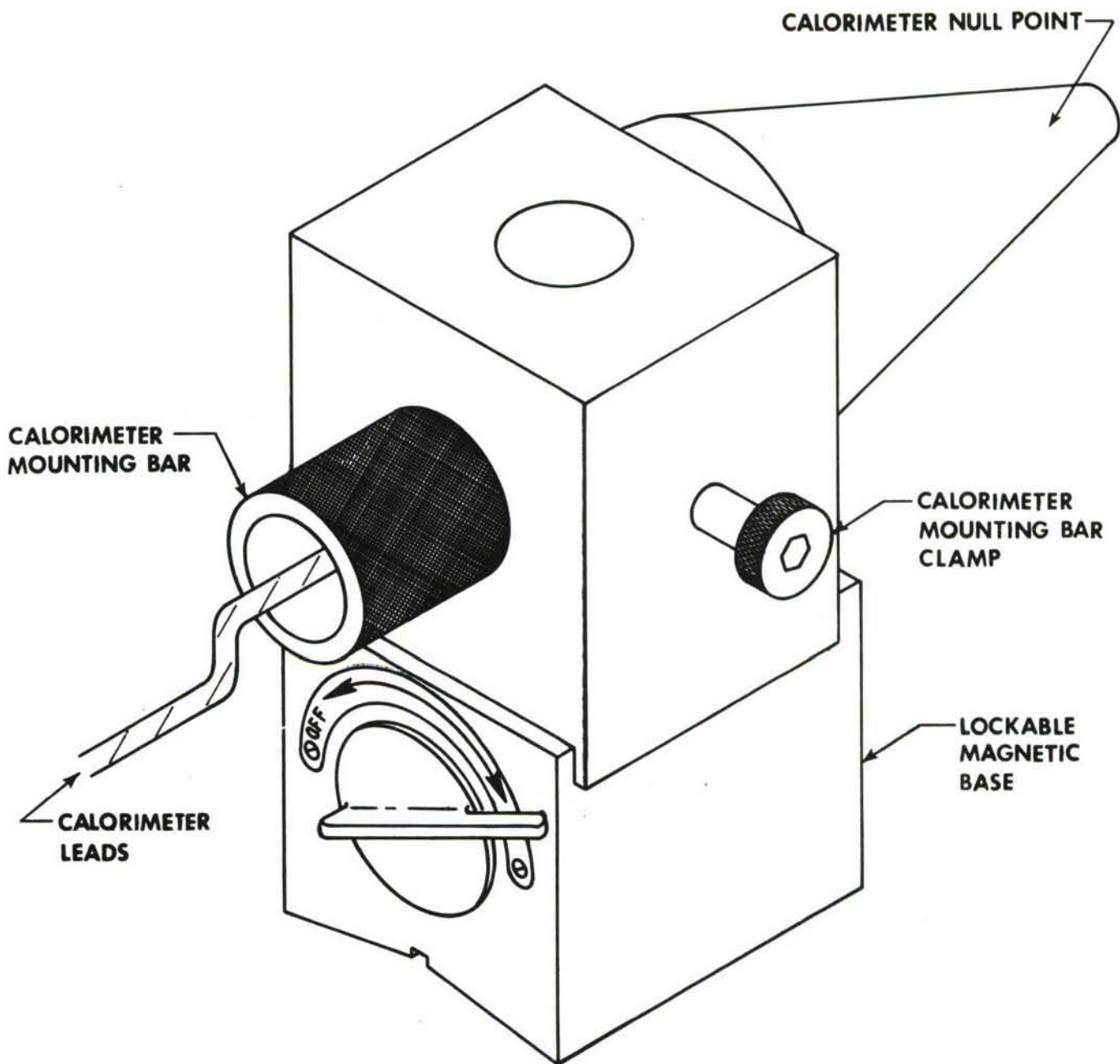


Figure 15 Null Point Calorimeter Mount



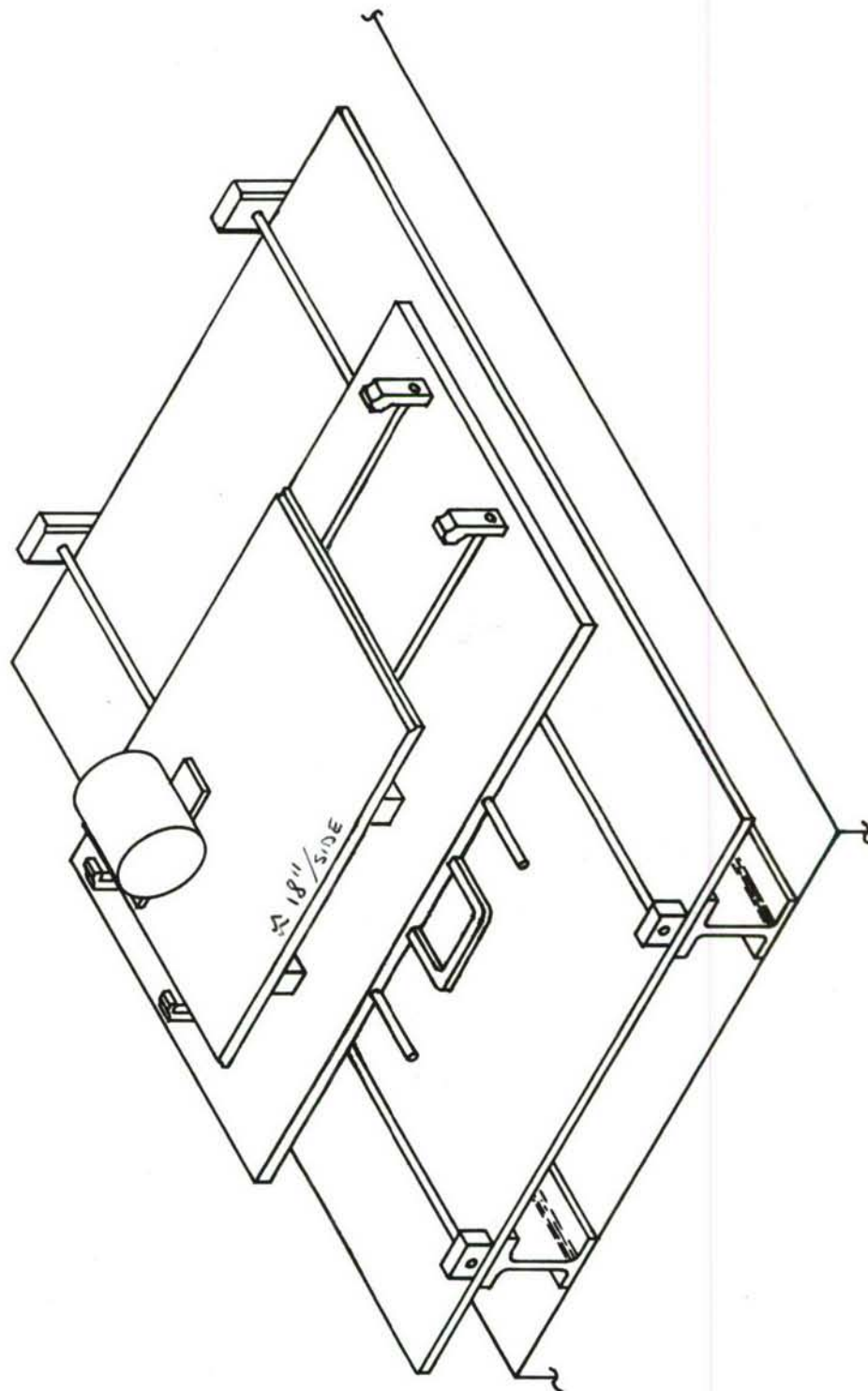


Figure 16 Table Assembly

## SECTION XII

### OVERALL SYSTEM PERFORMANCE

The overall system performance characteristics may be summarized as follows:

Very uniform (4%) heat flux densities can be generated through a 0.25 in. integrator up to  $10 \text{ kW/cm}^2$  ( $8,800 \text{ Btu/ft}^2\text{-s}$ ). Peak flux densities up to  $15 \text{ kW/cm}^2$  ( $13,000 \text{ Btu/ft}^2\text{-s}$ ) are available with the 0.25 in. aperture assembly. Graphs of the available flux densities are given in Figures 17 and 18.

The duration of the exposure can be automatically controlled from .01 to 9.99 seconds, or indefinitely in the manual mode. The characteristic rise and fall times are about 2 msec.

The flux density can be reliably and accurately measured with the transfer standard cavity radiometer which can be accurately calibrated for total input power. Present data on the aperture size effect appears to limit the accuracy of incident flux density measurements to about 4%. The present limit on damage threshold of the 0.125 in aperture is about  $8 \text{ kW/cm}^2$ , but it can be used up to about  $11 \text{ kW/cm}^2$  without melting. It may be possible to increase the threshold by employing a rhodium overcoating to increase surface reflectivity in the shorter wavelengths.

The absorptivity cavity provides a means of measuring the power absorbed by the detector. The absorptivity may be measured before and

UNIFORM HEAT FLUX PROVIDED  
BY  
0.25 x 0.25 OPTICAL INTEGRATOR

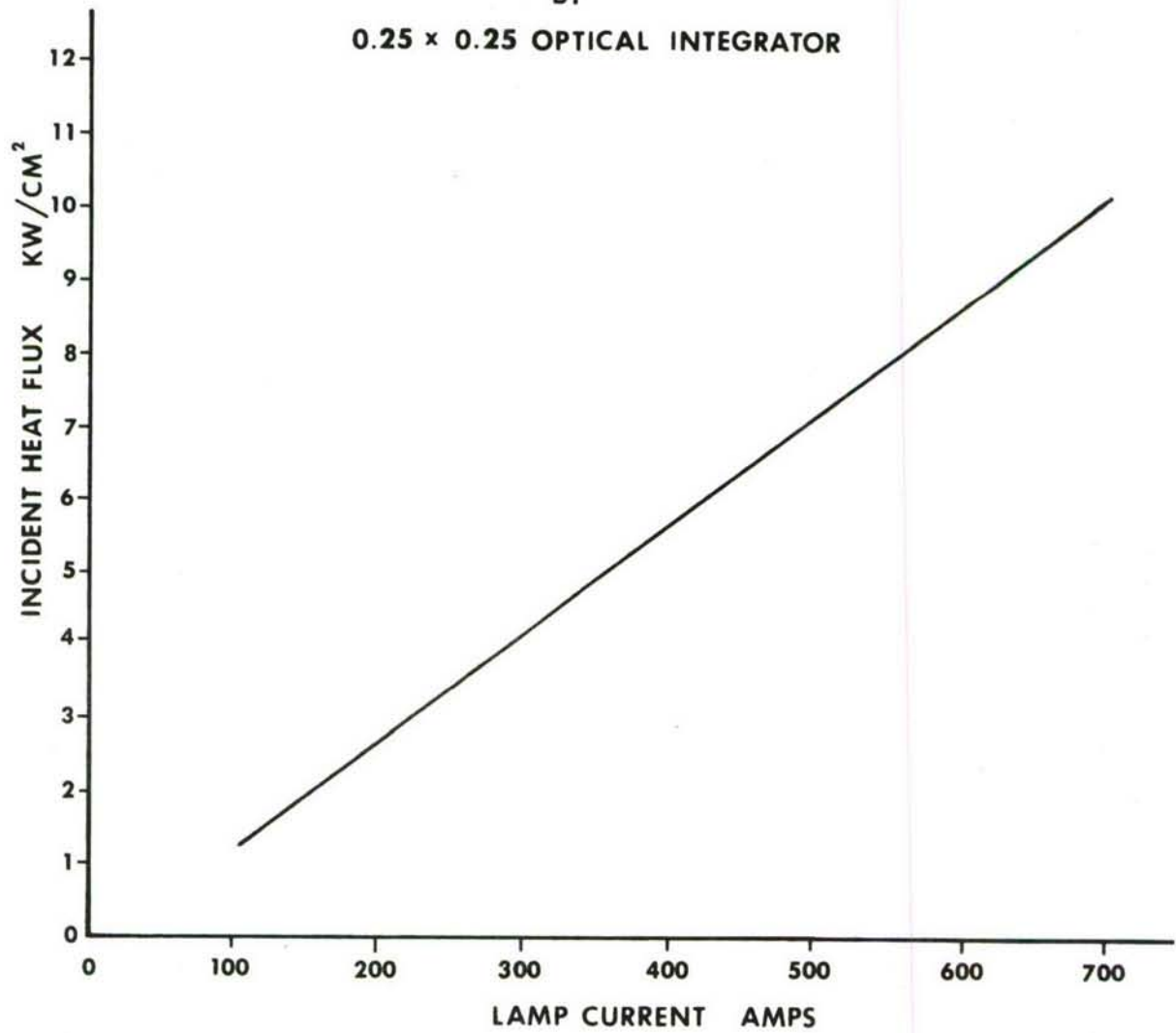


Figure 17 Uniform Heat Flux

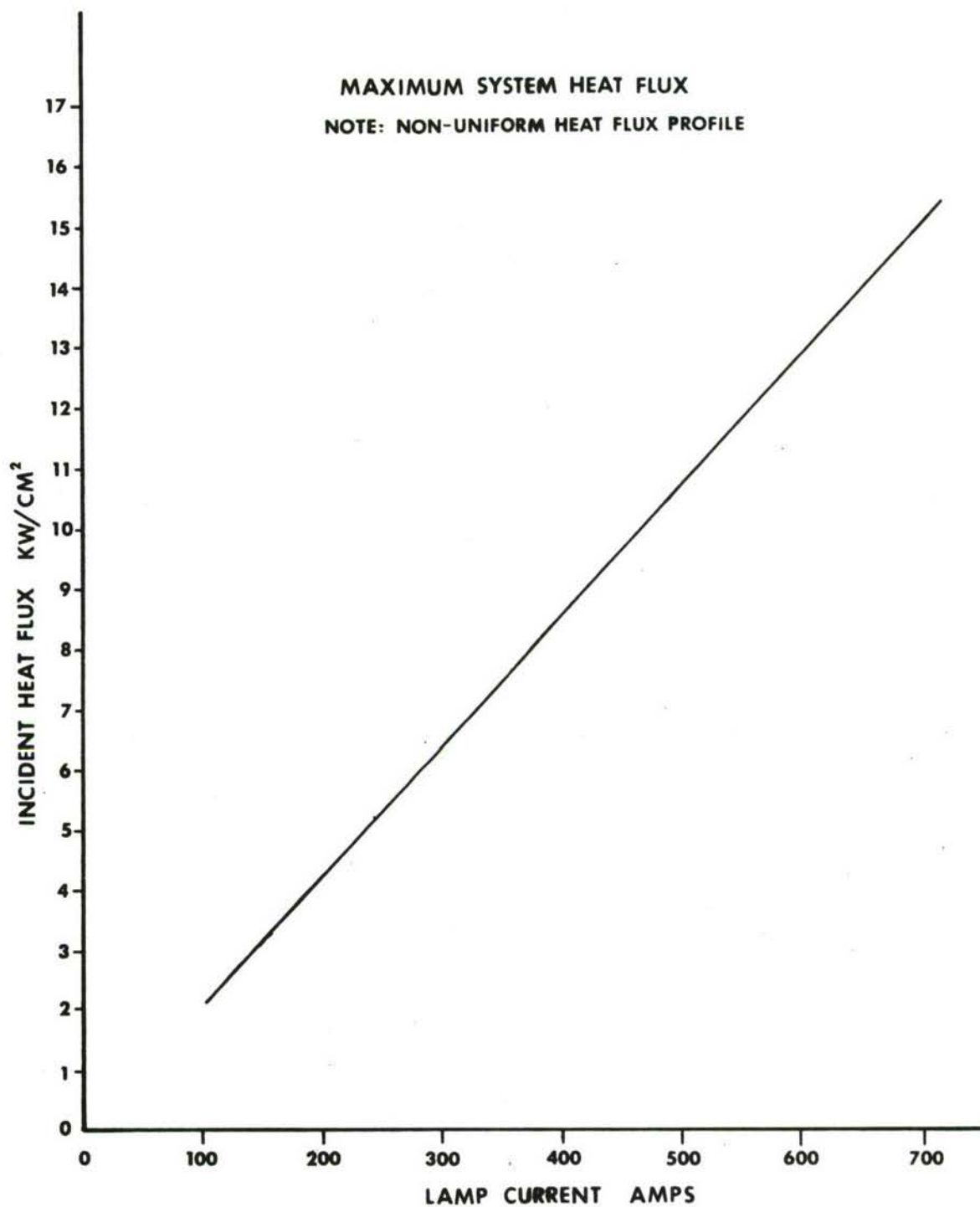


Figure 18 Maximum System Heat Flux

after exposure to ascertain changes that occur due to exposure. The assumption that the absorptivity of the colloidal graphite is relatively constant with flux level is borne by the agreement of data between the copper melt tests and radiometer data. The accuracy of the absorptivity measurements is about 2.5%.

With present data, the total calibration accuracy of the absorbed heat flux on a calorimeter is about 5% at uniform incident flux densities up to  $10 \text{ kW/cm}^2$ .

The system developed and delivered to the Air Force Flight Dynamics Laboratory is shown in Figure 19. It consists of the calibration module containing the source, radiometer and absorptivity device, a control console, a power supply and a small 400 Hz generator for the lamp xenon gas pump.



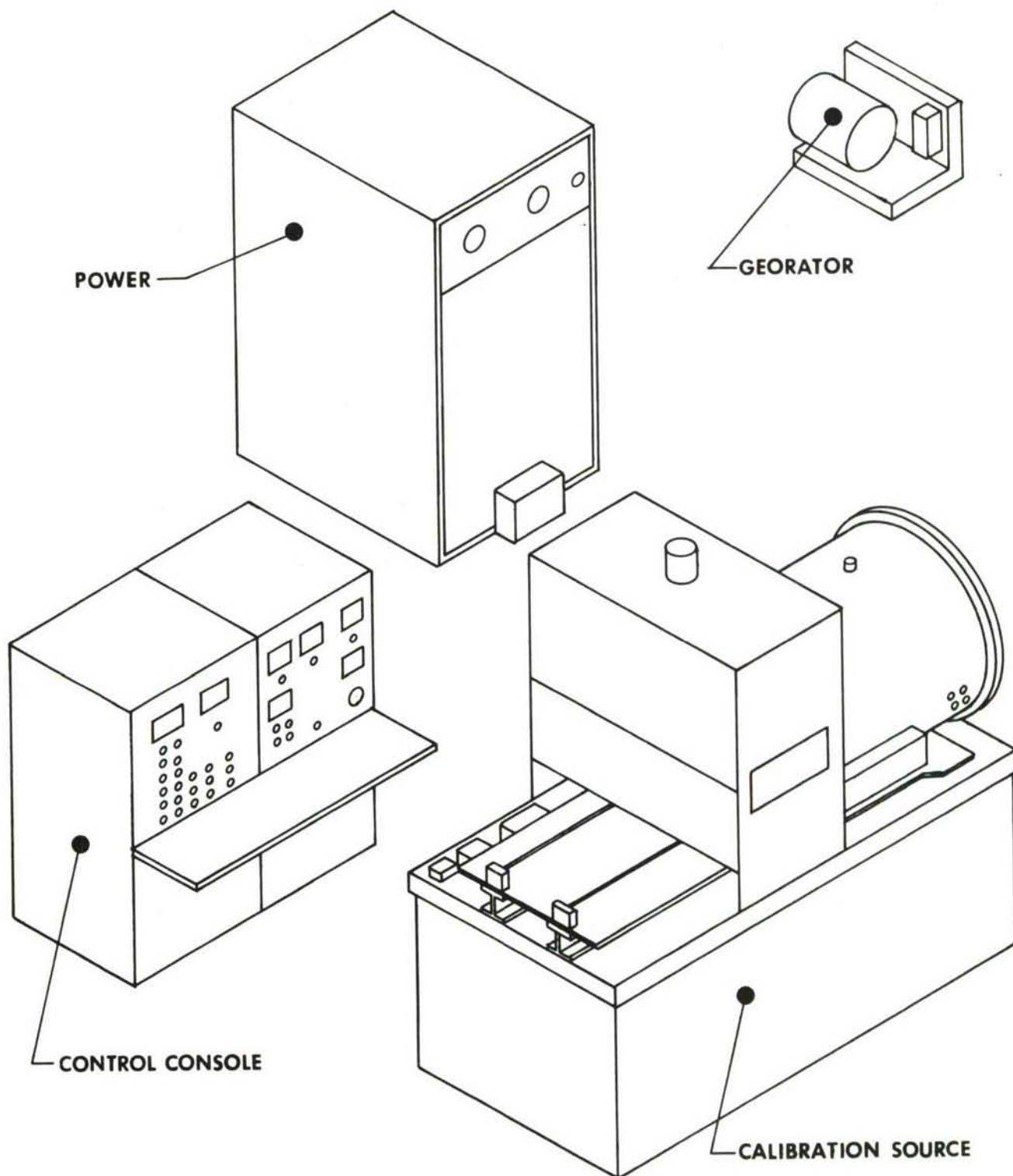


Figure 19 System Components